COMPUTATIONAL FLUID DYNAMIC (CFD) ANALYSIS OF A COLD-ADSORBED HYDROGEN TANK DURING REFILLING

D. Melideo[1], L. Ferrari[1], P. Taddei Pardelli[2]
[1] Department of Energy, Systems, Territory, and Construction, University of Pisa, Largo Lucio Lazzarino, 56122 Pisa, Italy
[2] Spike Renewables Srl, Viale Manfredo Fanti, 217, 50137, Firenze, Italy

ABSTRACT

Hydrogen has the potential to be an important source of clean energy, but the development of efficient and cost-effective methods for storing hydrogen is a key challenge that needs to be addressed in order to make widespread use of hydrogen as a possible energy sourc. There are different methods for storing hydrogen (i.e. compressed it at high pressures, liquefied by cooling the hydrogen to a temperature of -253°C and stored with a chemical compound), each with its own advantages and disadvantages.

MAST3RBoost (Maturing the Production Standards of Ultraporous Structures for High Density Hydrogen Storage Bank Operating on Swinging Temperatures and Low Compression) is a European project which aims to provide a solid benchmark of cold-adsorbed H2 storage (CAH2) at low compression (100 bar or below) by maturation of a new generation of ultraporous materials for mobility applications, i.e., H2-powered vehicles, including road and railway, air-borne and waterborne transportation. Based on a new generation of Machine Learning-improved ultraporous materials – such as Activated Carbons (ACs) and high-density MOFs (Metal-organic Frameworks) –, MAST3RBoost project will enable a disruptive path to meet the industry goals by developing the first worldwide adsorption-based demonstrator at the kg-scale.

The design of the tank is supported by numerical investigation by mean of the use of Computational Fluid Dynamic (CFD) commercial code. In this a paper a preliminary analysis of the refilling of tank is presented, focused on the effect of different tank configurations on the hydrogen temperature and on the hydrogen adsorption.

1.0 INTRODUCTION

The use of clean and renewable energy sources is increasingly important to reduce greenhouse gas emissions. Hydrogen is considered one of the most promising sources of energy in this regard [1], as it can be used as a vector of clean energy for the production of electricity and heat. However, one of the main obstacles to the diffusion of hydrogen is the shortage of efficient and safe systems for its storage [2], [3].

There are several different methods for storing hydrogen, each with its own advantages and disadvantages. One method for storing hydrogen is to compress it at high pressures, typically in the range of 350 – 700 bar. This method is relatively simple and inexpensive, but the tanks and equipment required to store hydrogen at these pressures can be heavy and bulky. Another method for storing hydrogen is to liquefy it by cooling it to a temperature of -253°C. This requires specialized equipment and insulation, but allows for the storage of hydrogen in a more compact form. A third method for storing hydrogen is to combine it with a chemical compound, such as metal hydrides or hydrocarbons. These compounds can store hydrogen in a solid form, but they may require special handling and may not be as efficient at storing hydrogen as the other methods.

The Department of Energy, Systems, Territory and Construction of the University of Pisa and Spike Renewables Srl, in the framework of the EU funded Project MAST3RBoost, are currently studying the cold-adsorbed H2 storage (CAH2) at low compression (100 bar or below); it is a promising technique, allowing to store hydrogen at high density with a reduction of volume. In particular this paper will

present the Computational Fluid Dynamic (CFD) results, considering the effect of the temperature and pressure on the hydrogen absorption, including also the effects of different type of adsorbents.

2.0 COLD-ADSORBED H2 STORAGE

An alternative approach to chemical hydrogen storage, is the adsorption of hydrogen using nonporous materials; in this case the molecules of hydrogen are physically adsorbed in the pores of substances having large surface areas and therefore extensive gas-solid interfaces, such as zeolites, activated carbons and metal-organic structures (MOF). That methodology allows to store hydrogen at lower pressure (i.e. 100 bar) compared to the compressed hydrogen storage and at higher temperatures (i.e. 77° K) compared to the ones adopted for the liquid hydrogen storage; compared to the chemical hydrogen storage, it has a quicker absorption and need lower temperature. At 77° K the amount of hydrogen adsorbed is predominant compared to the gaseous hydrogen inside the tank, especially at low pressure; that phenomena is strongly connected to the variation of pressure and temperature inside the tank [4]. In Figure 1 the density is reported as an increasing function of the storage pressure for different type of adsorbent material, and that this effect increases with decreasing temperature. The largest difference between the sorbent materials and the cryo-compressed case appears to be around 100 bar and 77 K, where the stored density of MIL-101 and compacted MOF-5 is 50% higher than for CcH2 (45 versus 30 kg/m3) [5].

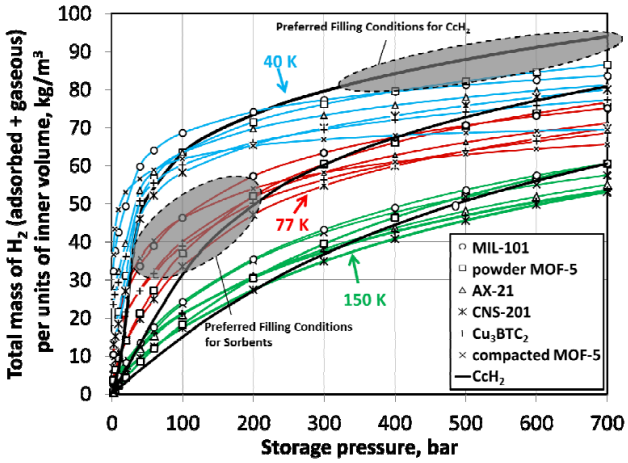

Figure 1. Total H2 density (including both adsorbed and gaseous phase) for different type of cryo-adsorbents

3.0 COMPUTATIONAL FLUID DYNAMIC (CFD) MODEL VALIDATION

The CFD model used for this study has been created with the commercial CFD code COMSOL Multiphysics 6.1 and compared against the experimental data (i.e. Test n. 20) [6, 7] and numerical results of filling of a 2.5 L tank with activated carbon [8]. An axial symmetrical mesh has been created and the temperatures calculated during the filling have been compared in some selected location as indicated in Figure 2

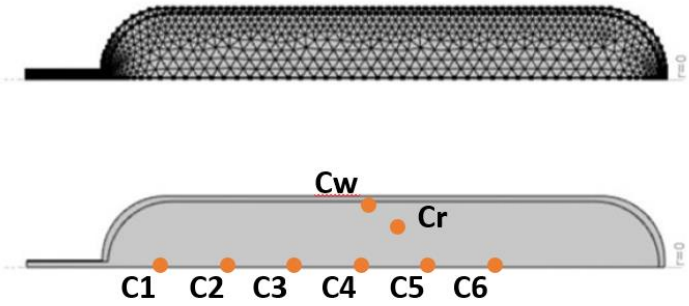

Figure 2. Computational grid and monitor point locations

The hydrogen storage tank is a stainless-steel container packed with adsorbents and is put into a Dewar flask filled with coolant (room temperature water or liquid nitrogen).

Material properties of hydrogen and tank are reported in Table 1, while the activated carbon properties are reported in Table 2

Table 1. Hydrogen and tank properties.

Properties	Hydrogen	Steel wall
Bulk density ρ_b kg/m^3	Ideal gas	7830
Specific Heat Cp J/kgK	14700	468
Conductivity k W/mK	0.206	13
Dynamic viscosity μ Pa·s	8.411e-6	-

Table 2. Activated Carbon properties.

Properties	Activated Carbon
Bulk density ρ_b kg/m^3	269
Specific Heat Cp J/kgK	825
Conductivity k W/mK	0.764
Bed porosity ϵ	0.49
Particle diameter d_p mm	2.0

A modified Dubinine-Astakhov (MDA) adsorption model [9] is used to describe the adsorption isotherm for MOF-5 and activated carbon (AC). The absolute adsorption is given by the following equation:

$$n_a = n_{max} \exp\left[-\left(\frac{RT}{\alpha_{D-A} + \beta_{D-A} T} \ln \frac{p_0}{p} \right)^m \right] \qquad \text{Eq. 1}$$

Where R is the universal gas constant, T and p are the temperature and pressure, respectively. The exponent m is allowed to vary and is normally between 1 and 2 for adsorption of various gases on most adsorbents, and for hydrogen adsorption on MOF-5 and activated carbon, m equals to 2. The specific value used in Eq. 1 are the ones reported in Table 3

Table 3. MDA parameters for AC.

Parameters	Activated Carbon
n_{max} mol/kg	71.6
P_0 MPa	1470
α J/mol	3080
β J/molK	18.9

The tank is at 0.03208 MPa and 302º K as initial pressure and temperature. The tank is cooled using water at 302.5º K and the heat transfer coefficient between steel wall and room temperature water is 36 W/(m^2 K). The hydrogen in entering the tank with at 2.048e-05 kg/s and the filling time is 953 s.

The pressure profile calculated inside the tank is in agreement with the experimental data and reported in Figure 3; the maximum pressure reached inside the tank at the end of the filling is 9 MPa.

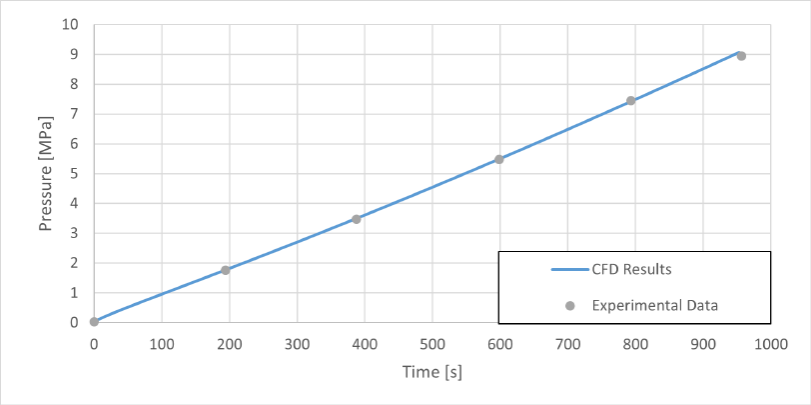

Figure 3. Pressure profile during the filling compared with the experimental data

In Figure 4 the temperature profile during the filling at different location along the axis of the tank are compared with the experimental data; the CFD results are in agreement with the experimental data and, with the exception of C1 (i.e. the point located close to the inlet of the tank) the CFD results tend to underestimate the experimental data.

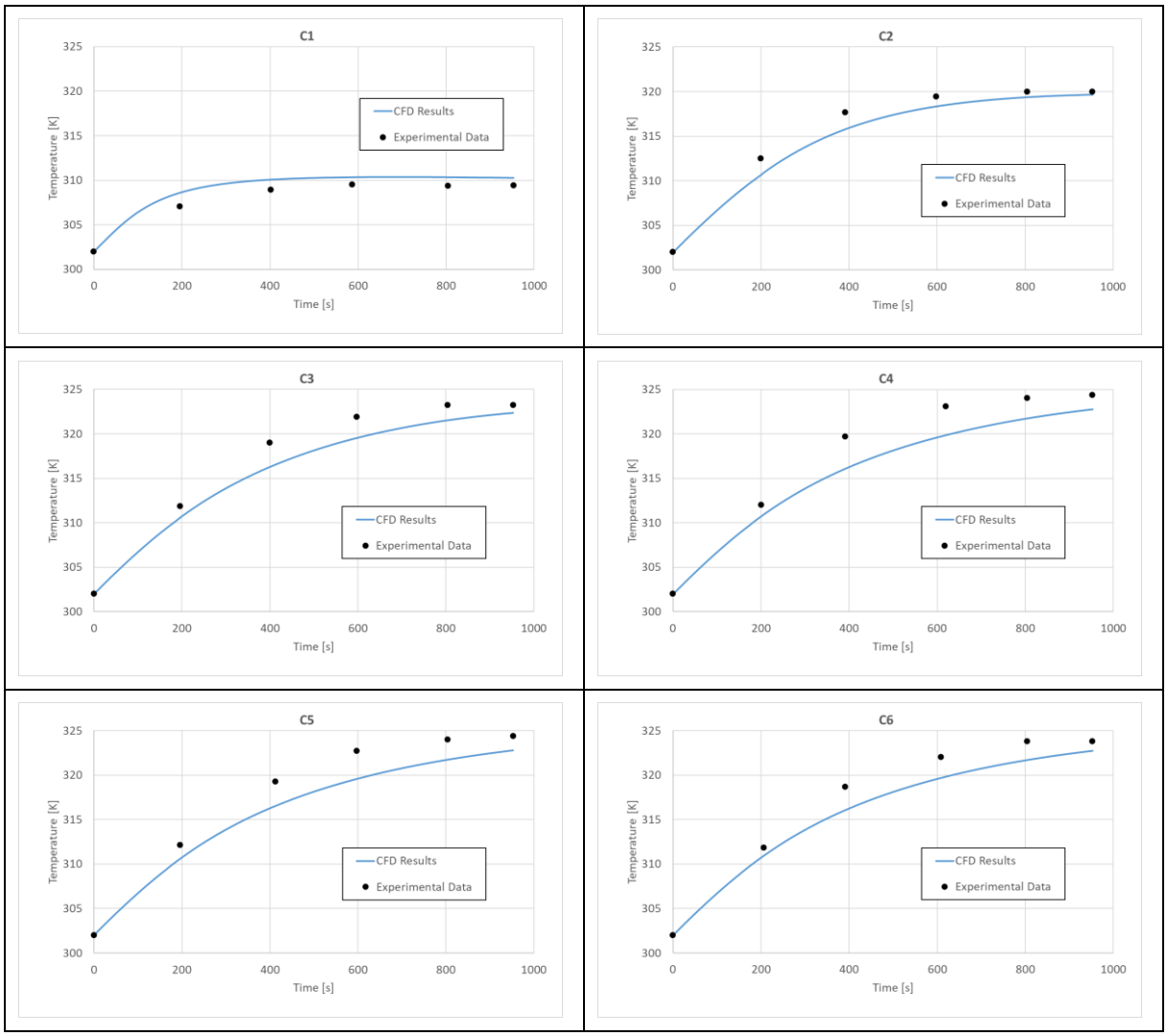

Figure 4. Temperature profile at selected locations during the filling compared with the experimental data

In Figure 5 the temperature profile during the filling at different location close to the wall of the tank are compared with the experimental data; also in this case, the CFD results are in line with the experimental data; point Cw seems not to follow the trend of the experimental value towards the end of the filling, probably due to use of a non-accurate heat transfer coefficient between steel wall and room temperature water.

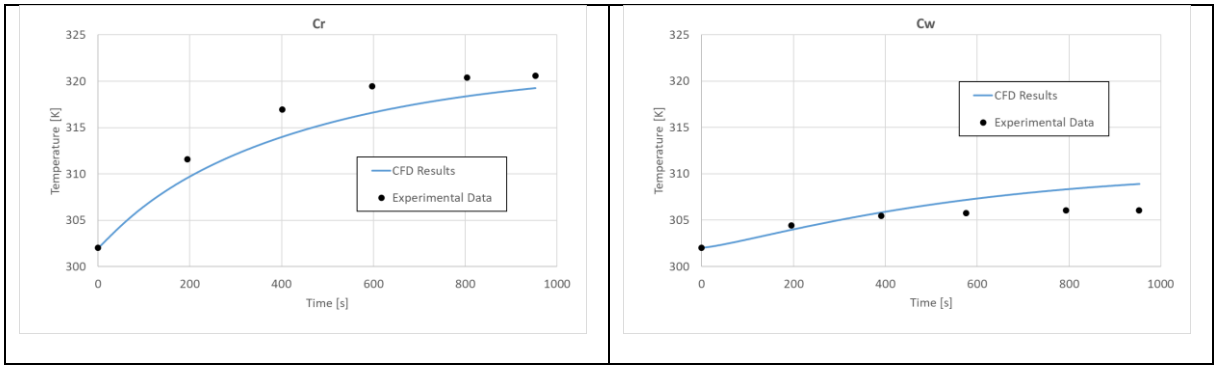

Figure 5. Temperature profile at selected locations close to the tank wall during the filling compared with the experimental data

The gaseous hydrogen mass and the adsorbed hydrogen mass at the end of the filling are 8.7g and 11g respectively; those values are in line with the one calculated in [8], which are 8.7g and 11.2g respectively.

In Figure 6 the temperature contours (left-hand side) and the absolute absorption (right-end side) at the end of the filling are reported; it can be noted the lower is the temperature, the higher is the absorption of hydrogen.

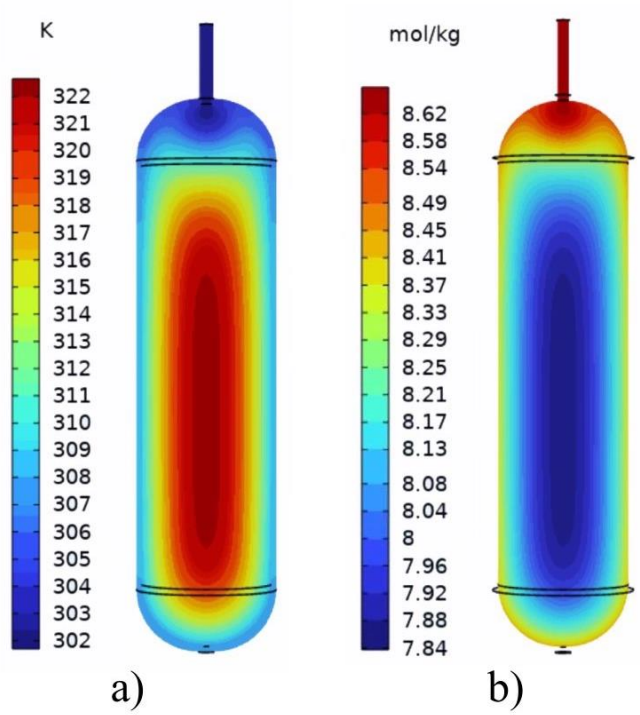

Figure 6. Temperature contours (a) and absolute adsorption (b) at the end of the filling

4.0 EFFECT OF DIFFERENT INITIAL TANK AND HYDROGEN INLET TEMPERATURE

The CFD model has been then used to simulate the filling of the tank in presence of AC with different inlet hydrogen temperature (i.e. 77º, 150º and 233º K) at different initial tank temperature (i.e. 233º, 150º and 77º K). The mass of hydrogen inside the tank at the end of the filling (i.e. 500s) for the different configurations is reported in Figure 7; for each hydrogen inlet temperature (i.e. T inlet in figure), the effect of the different initial temperature is reported (i.e. TO in figure): the lower is the temperature (either the initial and the inlet temperature), the higher is amount of hydrogen stored in the tank. The share of adsorbed hydrogen by the AC is also reported with the fill pattern for each case in Figure 7; it can be observed than more than half of the total hydrogen stored in the tank is adsorbed by the AC for all the cases.

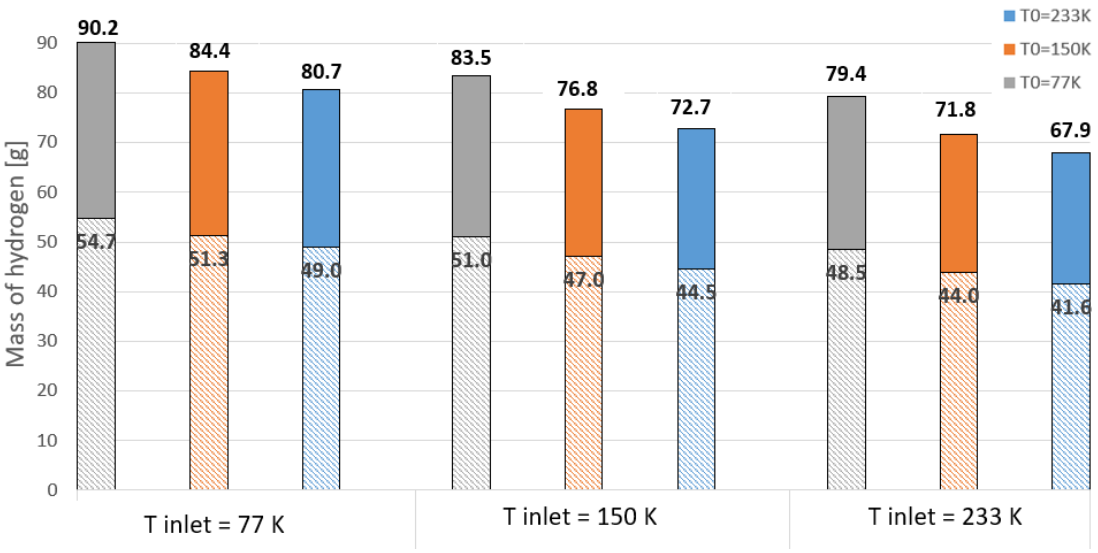

Figure 7. Adsorbed and total hydrogen mass at the end of the filling for different configurations

The adsorption contours in [mol/g] at the end of the filling are reported in Figure 8 for all the configuration studied.

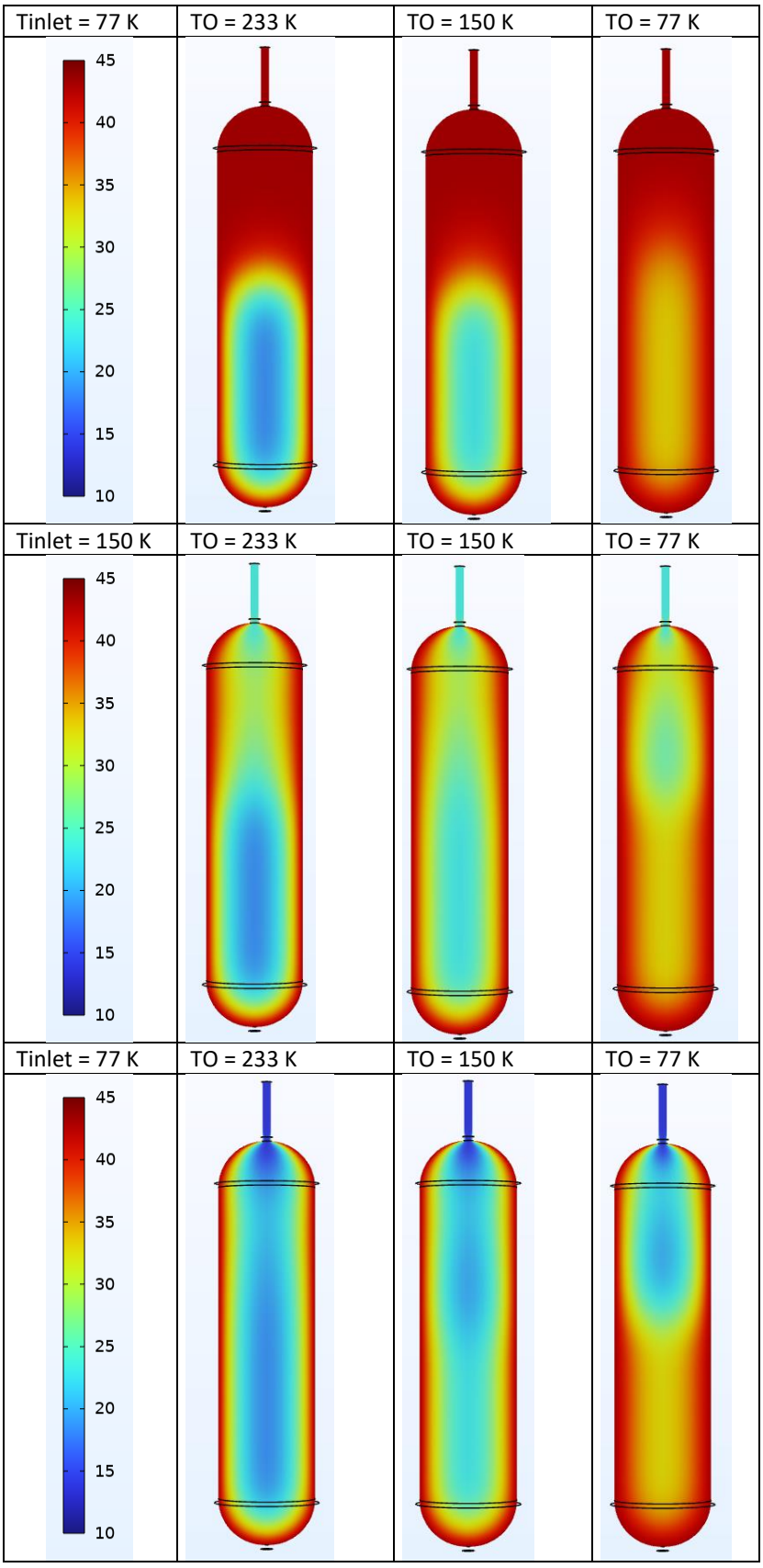

Figure 8. Adsorption [mol/Kg] inside the tank at the end of the filling

5.0 EFFECT OF PRESSURE RAMP RATE

The effect of different pressure ramp rate on the final hydrogen mass stored has been considered. As reported in Figure 9, two cases have been studied considering to reach the target pressure of 10 MPa with two different rising time, 15 s and 45 s respectively; the initial tank temperature and the hydrogen inlet temperature are 77º K both.

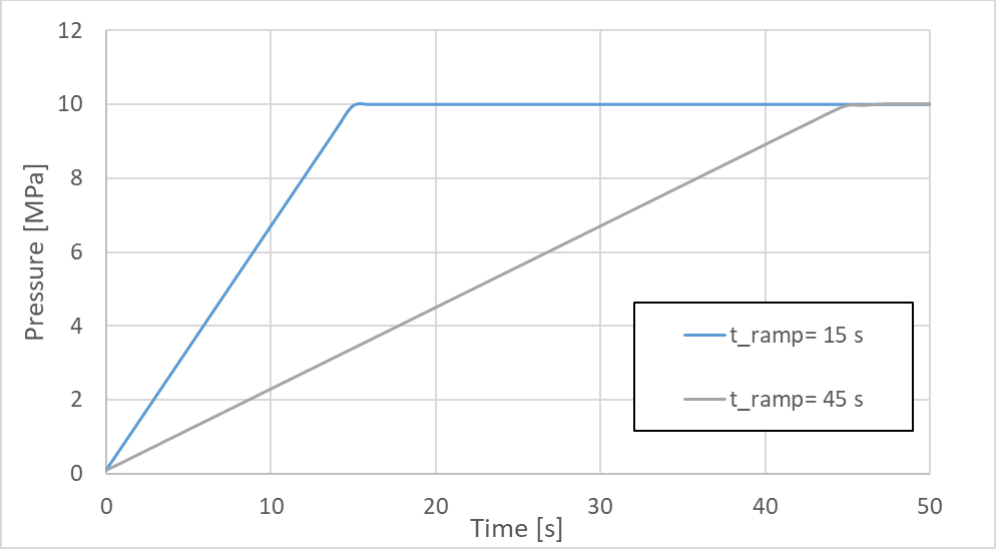

Figure 9. Pressure profile for the two studied cases

The temperature profile calculated in the C1 and C6 locations are reported in Figure 10; the use of different pressure ramps slightly affects the temperature only at the beginning of the filling process, while the pressure is increasing.

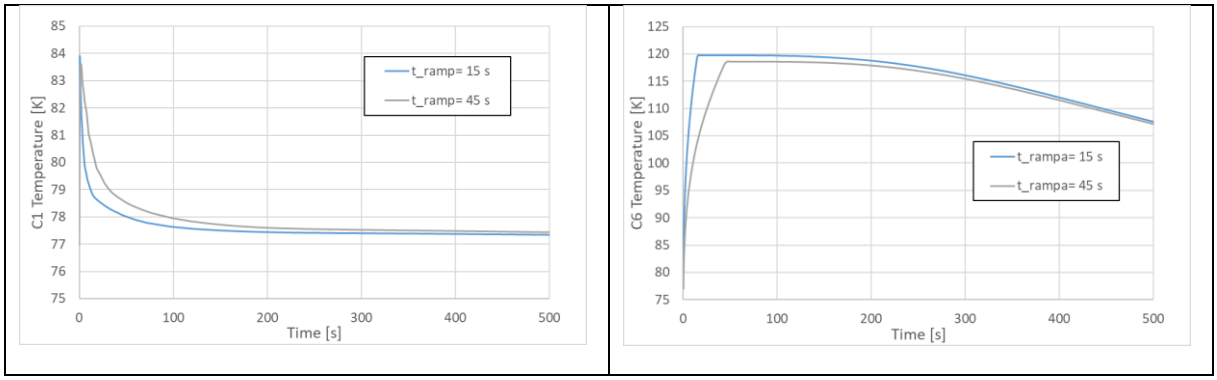

Figure 10. Temperature profile at C1 (left) and C6 (right) for the two different adopted pressure ramps

It has been calculated the use of different inlet pressure profile does not affect the amount of hydrogen stored in the tank at the end of the filling.

6.0 THE USE OF DIFFERENT ADSORBENT MATERIALS

The effect of two different types of adsorbent materials (i.e. activated carbon and compacted MOF-5) on the final hydrogen stored has been calculated, considering a filling time of 500 s, a pressure ramp of 15 s, and 77º K as initial tank temperature and inlet hydrogen temperature. The adsorbent material properties considered for the simulation are reported in Table 4.

Table 4. Activated Carbon (AC) and compacted MOF-5 properties [10].

Properties	Activated Carbon	Compacted MOF-5
Bulk density ρ_b kg/m^3	269	406
Specific Heat Cp J/kgK	825	742.5
Conductivity k W/mK	0.764	0.3
Bed porosity ϵ	0.49	0.1266
Particle diameter d_p mm	2.0	0.038
Permeability m^2	1.7e-08	2e-13

The parameters adopted for MDA implemented in the CFD code are reported in Table 5.

Table 5. MDA parameters for AC and compacted MOF-5 [8].

Parameters	Activated Carbon	Compacted MOF-5
n_{max} mol/kg	71.6	70.178
P_0 MPa	1470	1927.3
α J/mol	3080	2541.5
β J/molK	18.9	8.0691

The temperature profile calculated in the C1 and C6 locations are reported in Figure 11. It can be observed how the use of different adsorbent material affects the temperature inside the tank during the filling: the tank with compacted MOF-5 has higher temperature compared to the tank with AC; this effect is probably related to the different heat transfer coefficient and density of the two adsorbents; at the end of the filling the temperatures calculated in the two selected point are almost the same for the two cases.

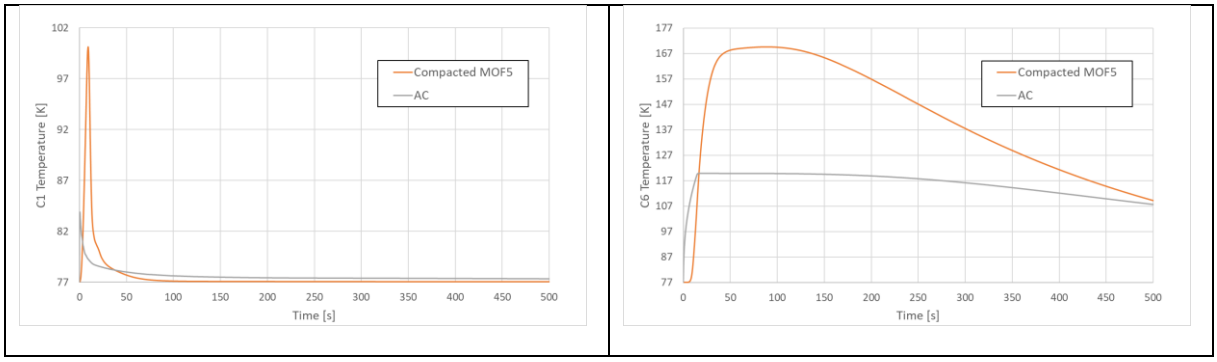

Figure 11. Temperature profile at C1 (left) and C6 (right) for the two different adsorbent materials

The contours of temperature (left hand side) and absolute adsorption (right hand part) for AC and MOF-5 at the end of the filling are reported in Figure 12. The use of AC gives a more diffuse high temperature zone compared to the use of MOF-5, where the hot spot is located more towards the end of the tank (i.e. the opposite side with respect to the inlet tube); as a consequence, also the absolute adsorption distribution has the same trend.

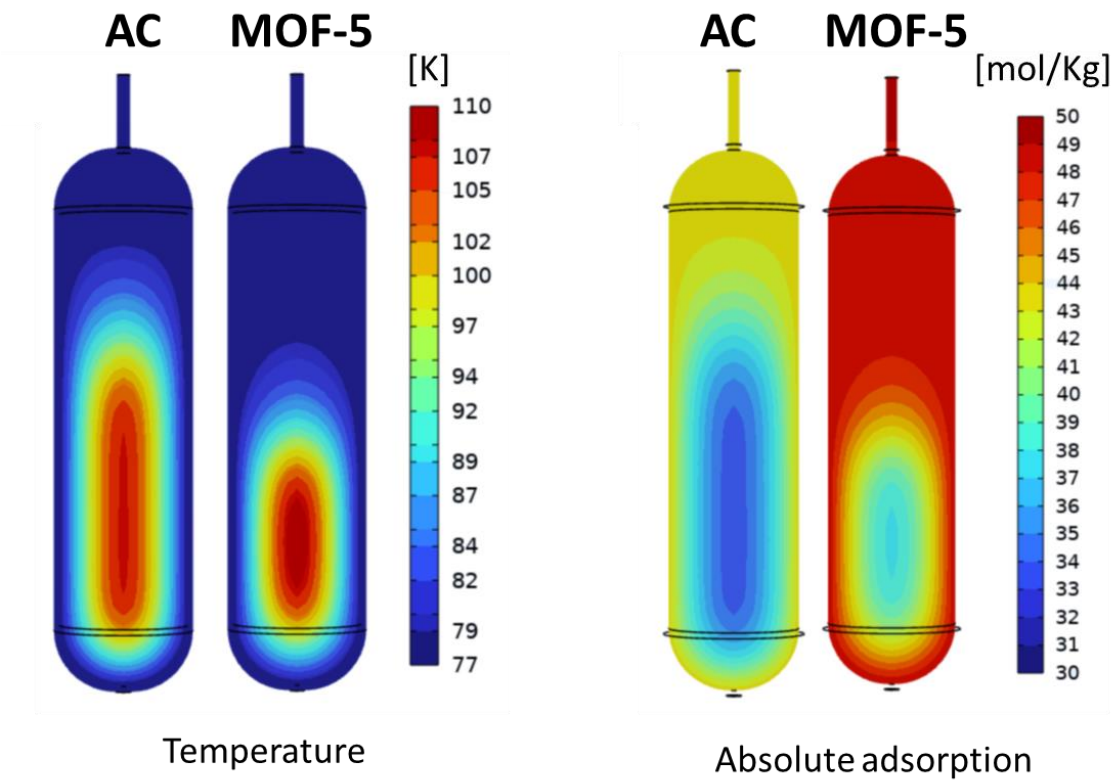

Figure 12. Contours of temperature (left part) and absolute adsorption (right part) for AC and MOF-5

The amount of hydrogen inside the tank at the end of the filling and the share of adsorbed hydrogen (indicated with the fill pattern) by the AC and by the MOF-5 is reported in Figure 13. It can be observed how the use of MOF-5 increases the amount of adsorbed hydrogen compared to the use of AC: almost the whole amount of hydrogen entering the tank is adsorbed by MOF-5 (i.e. 95.4 g of hydrogen adsorbed out of 104 g of the total amount of hydrogen inside the tank at the end of the filling).

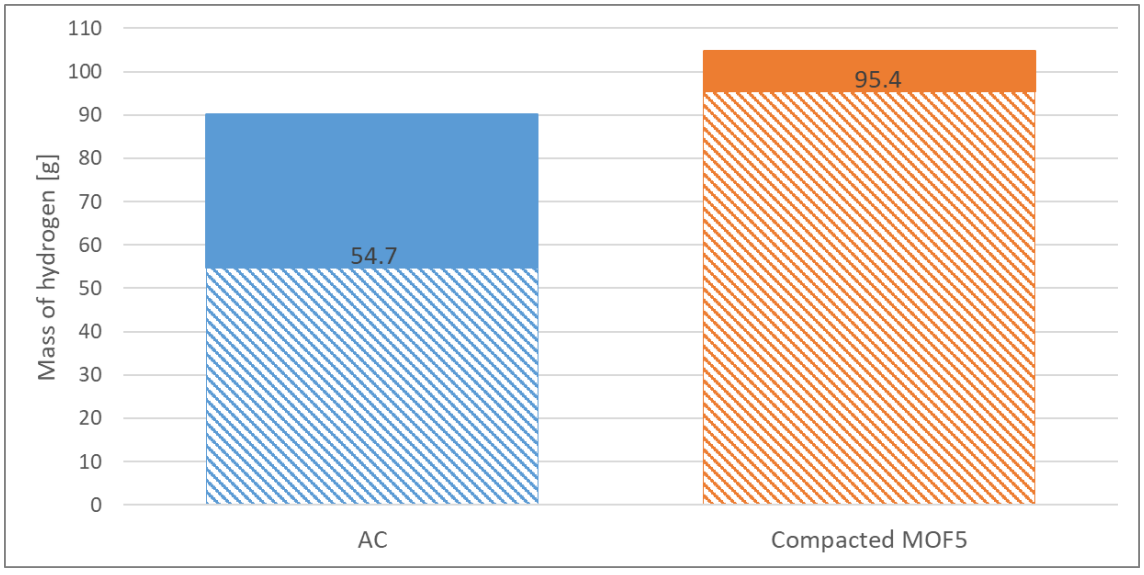

Figure 13. Adsorbed and total hydrogen mass at the end of the filling for AC and MOF-5

CONCLUSIONS

A CFD model simulating the filling of hydrogen tank in the presence of adsorbent material has been validated and used to study the effect of the inlet temperature, inlet pressure ramp rate and initial tank temperature on the amount of hydrogen stored at the end of the filling; the lower is the temperature the higher is the absolute absorption of the hydrogen. The effect of two type of adsorbent material (i.e. AC and MOF-5) have been also studied: for the case studied, MOF-5 has higher absolute adsorption than the AC.

ACNKOWLEDGEMENT

Funded by the European Union

MAST3RBoost is a funded by the European Union. Views and opinions expressed are however those of the author(s) only and do not necessarily reflect those of the European union or the European health and digital executive agency. neither the European union nor the granting authority can be held responsible for them.

Project funded under the National Recovery and Resilience Plan (NRRP), Mission 4 Component 2 Investment 1.3 - Call for tender No. 1561 of 11.10.2022 of Ministero dell'Università e della Ricerca (MUR); funded by the European Union – NextGenerationEU

REFERENCES

[1] IEA (International Energy Agency). The Future of Hydrogen. Rep Prep by IEA G20, Japan 2019. https://doi.org/10.1787/1e0514c4-en.

[2] Rivard E, Trudeau M, Zaghib K. Hydrogen storage for mobility: A review. Materials (Basel) 2019;12. https://doi.org/10.3390/ma12121973.

[3] Tzimas E, Filiou C, Peteves SD, Veyret J. Hydrogen Storage : State-of-the-Art and Future Perspective. 2003.

[4] Sdanghi G, Schaefer S, Maranzana G, Celzard A, Fierro V. Application of the modified Dubinin-Astakhov equation for a better understanding of high-pressure hydrogen adsorption on activated carbons. Int J Hydrogen Energy 2020;45:25912–26. https://doi.org/10.1016/j.ijhydene.2019.09.240.

[5] Petitpas G, Benard P, Klebanoff LE, Xiao J, Aceves M. A Comparative Analysis of the Cryo-compression and Cryo-adsorption Hydrogen Storage Methods 2014.

[6] Xiao J, Wang J, Cossement D, Bénard P, Chahine R. Finite element model for charge and discharge cycle of activated carbon hydrogen storage. Int J Hydrogen Energy 2012;37:802–10. https://doi.org/10.1016/j.ijhydene.2011.04.055.

[7] Xiao J, Peng R, Cossement D, Bénard P, Chahine R. CFD model for charge and discharge cycle of adsorptive hydrogen storage on activated carbon. Int J Hydrogen Energy 2013;38:1450–9. https://doi.org/10.1016/j.ijhydene.2012.10.119.

[8] Xiao J, Hu M, Bénard P, Chahine R. Simulation of hydrogen storage tank packed with metal-organic framework. Int J Hydrogen Energy 2013;38:13000–10. https://doi.org/10.1016/j.ijhydene.2013.03.140.

[9] Chahine MRPBR. Gas adsorption process in activated carbon over a wide temperature range above the critical point . Part 1 : modified Dubinin-Astakhov model 2009:43–51. https://doi.org/10.1007/s10450-009-9149-x.

[10] Henning Lohse-Busch, Kevin Stutenberg. Toyota Mirai Testing; DOE Hydrogen and Fuel Cells Program FY 2018 Annual Progress Report. 2018.